Chemistry and Materials Research
ISSN 2224- 3224 (Print) ISSN 2225- 0956 (Online)
Vol.6 No.10, 2014

Synthesis and Photocatalytic Activity of Single Crystal Titanate: Part-1

Amr Nada (Corresponding author)
Egyptian Petroleum Research Institute, EPRI, Cairo, Egypt
E-mail: chem_amr@yahoo.com

Yasser Moustafa and Amal Hamdy
Egyptian Petroleum Research Institute, EPRI, Cairo, Egypt

Saad Abd El-Wahab and Dena Yahea
Ain shams Univeristy Cairo, Egypt.

Abstract
Single crystal TiO_2 nanotubes (TNTs) were prepared using modified hydrothermal method by treatment of prepared TiO_2 with NaOH aqueous solution and characterized by the X-ray diffraction (XRD), high-resolution transmission electron microscopy (HRTEM), thermogravimetric (TG) analysis, BET surface area analysis, Raman spectroscopy, FTIR and UV–vis/DR spectroscopy. Detailed study for the effect of calcinations temperature on the morphology, textural properties, adsorption amount and photocatalytic activity of TiO_2 nanotubes was performed. The results showed that the calcinations temperature remarkably altered the phase composition. HRTEM showed that the high-purity nanotubes can be produced through the hydrothermal treatment of TiO_2, calcinated at 250 ^oC. It was found that the obtained high-purity TNTs have outer diameter of the tubular structures around 15 nm and the length is around 70 nm, the wall of nanotube is 2 layers in one side whereas it is 3 layers in another side and the interlayer spacing is about 1–1.5 nm. The prepared TiO_2 nanotubes show enhanced catalytic activity in photocatalytic phenol degradation compared with TiO2 nanoparticles which show lower catalytic activities.
Keywords: Titanate, Single Crystal, hydrothermal method

1. INTRODUCTION

Nanoscale structures have attracted immense interest in recent years. Especially, single crystal nanotubes are of particular interest owing to their unique atomic structures and great potential in electronic, optical, mechanical, and bioscience applications (Nalwa et al., 2000). In recent years, TiO_2 nanotubes (TNTs), a novel single crystal nanostructured material, has been attracting considerable attention because of their superior properties relative to conventional bulk materials. The TNTs can be prepared by different methods, including the template method (Sun et al., 2011), anodic oxidation and the alkaline hydrothermal method (Ou and Lo, 2007). Among these approaches, the alkaline hydrothermal method reported by Kasuga et al. (1998, 1999) is a facile and environmentally friendly technology, which was obtained by the reaction of TiO_2 powder with highly concentrated NaOH solution, subsequently treated with acid solution, Compared with the template method and anodic oxidation processes, hydrothermal method is easy to operate with high quality and high yield (Bavykin et al., 2006).

The photocatalytic degradation is an important chemical process, which utilizes the photo-generated holes and electrons to decompose the organic pollutants. Titanium-based nanomaterials (Aqeel and Ali, 2013), i.e. titanium oxides (TiO_2) and titanates, as the most promising photocatalysts, have obviously attracted extra attention in the degradation of dye pollutants originating from their unique properties of chemical inertness, high photoreactivity, non-toxicity, and photostability (Chen and Mao, 2007 & Zhang et al., 2010). The crystal phase and particle size of titanium-based photocatalysts are well known key factors to their photocatalytic activity.

In this contribution, the high-yield TNTs with various morphologies were prepared by the modified hydrothermal method followed by well-controlled calcination. The effects of calcination temperature on the phase structure, crystallization, morphology and specific surface area were studied. The photocatalytic activities of the TNTs were evaluated by photocatalytic degradation of phenol. This work may provide a basis for the applications of TNTs material in environmental purification.

2. EXPERIMENTAL

2.1. Preparation of TiO_2 nanoparticles

All chemicals were of analytical grade and used without further purification.TiO_2 nanoparticles were prepared by the method of hydrolysis as reported by (S.S. Kanmani and K. Ramachandran, 2012) with little modification. Titanium (IV) isopropoxide ($Ti[OCH(CH_3)_2]_4$) was used as a starting precursor. Typically, 5 ml of $Ti[OCH(CH_3)_2]_4$ was dissolved in 100 ml of isopropyl alcohol [$(CH_3)_2CHOH$] and solution was stirred

continuously for 1 h at room temperature. After stirring, 400 ml of deionized water was added suddenly to the above prepared mixture. The resultant solution was aged for 3 h, then centrifuged, washed several times with deionized water and ethanol and dried at 80 °C over night. The preparation of the TiO_2 nanoparticles was then completed by calcinating the precipitated particles at 450 °C for 2 h in air.

2.2. Preparation of TiO_2 nanotubes (TNTs)

TNTs were prepared by the modified hydrothermal method (Li 2009). In a typical run, 2 g TiO_2 powder was added into 50 mL of 10 mol/L NaOH aqueous solution and the suspension system was stirred for 1 h at room temperature to form a suspension. Then, the mixture was transferred to a Teflon-lined stainless steel autoclave at 130 °C for 24. After cooled naturally in air, the mixture was centrifuged at a speed of 4000 rpm and the precipitates were collected. The white powder was thoroughly washed with water then with 0.1M HCl, followed by drying at 80 °C. Nanotube samples with different properties were prepared by calcining the as-prepared nanotube at corresponding temperatures for 4 h with an increment of 1 °C/min. The resulting TiO_2 nanotube catalysts are labeled as TNT-x (x denotes the calcination temperature, and TNT-un refers to the nanotube uncalcined).

2.3. Characterization of TiO_2 nanotube

The studied samples were examined using X-ray powder diffractometer, Panalytical XPERT PRO MPD. Cu Kα radiation (λ= 1.5418 A°) was used at a rating of 40 kV, 40 mA. The diffraction patterns were recorded at room temperature in the angular range of 4°-80° (2θ) with step size 0.02° (2θ) and scan step time 0.4 (s). The crystalline phases formed on the carbon steel surface, in bothcases, were identified using the ICDD-PDF database.

The thermogravimetric (TG) analysis of the sample was conducted on a Q600 DST simultaneous DSC/TGA apparatus. All runs were carried out at a heating rate of 10ºC/min in the temperature range from room temperature to 1000ºC.

High Resolution Transmission Electron Microscopic (HRTEM) images were obtained with a JEOL-1400 TEM at 200 kV.

The specific surface areas of the samples were determined by N_2 adsorption-desorption isotherms at liquid nitrogen temperature (-196 ºC) using Quantachrome Nova 3200 S automates gas sorption apparatus.

Raman spectra of samples were recorded on the dispersive Raman microscope Sentera Bruker instrument at laser wave length 532 nm and power 10 mW.

Fourier transform infrared spectroscopy (FT-IR) spectra on the pellets of the samples were recorded on a Perkin-Elmer FT-IR spectrometer.

UV–VIS/DR spectra were recorded using Jasco V 530 spectrometer (Japan) equipped with the integrating sphere accessory for diffuse reflectance spectra.

X-ray photoelectron spectroscopy (XPS) was recorded with Perkin Elmer PHI 5000C ESCA System with Al Kα radiation operated at 250 W.

2.4. Photocatalytic reactions

Photocatalytic reactions were conducted in a commercial photo-reactor equipped with a 500 ml cylindrical Pyrex vessel irradiated directly by a high pressure mercury lamp (125 W). For photocatalytic phenol degradation, 0.2 g of the catalyst was mixed with 500 ml of 50mg/l phenol solution which was further stirred in the dark for 30 min to reach the adsorption equilibrium prior to the photocatalytic test. During the photocatalytic reaction, samples were collected at selected time intervals and the catalyst particles were removed by centrifugation. The residual phenol concentration was determined using HPLC (Agilent 1200, USA), equipped with an ultraviolet (UV) detector and a C18 reversed phase column (250mm×4.5mm, Agilent, USA) at 30 °C. The mobile phase consists of water and acetonitrile (40/60, v/v) with a flow rate of 1.0 ml min^{-1}.

3. RESULTS AND DUSCUSSION

3.1. Structural characterization

The X-ray diffraction patterns of prepared TiO_2 nanoparticles calcined at 450 °C for 2 h, TiO_2 nanotubes uncalcined and calcined at different temperatures for 4 h, shown in fig. 1,. can be seen that the calcination temperatures obviously influence on the crystallization and phase structures of the TNTs samples. For 250 and 350 °C calcined samples, weak diffraction peaks were observed with 2Θ at 24.54°, 28.4° and 48.1°, attributed to single crystal monoclinic titanate $H_2Ti_3O_7 \cdot xH_2O$ (Lin et al. 2008). The generation of titanate under alkaline hydrothermal conditions is based on a dissolution recrystallization mechanism, by which TiO_2 precursor is irreversibly converted into soluble titanate species and these species are further thermodynamically deposited and crystallized into lamellar titanate (Morgado et al. 2007 & Wu et al. 2006). With increasing calcination temperatures (from 350 to 650 °C), also for TiO_2 nanoparticles, new diffraction peaks were observed at 25.5°,

37.8◦, 48.2◦, 54.2 and 55.4◦, assigned to metastable polymorph TiO_2 (Feist et al. 1988). XRD peak intensities of anatase steadily become stronger and the width of XRD diffraction peaks of anatase becomes narrower, indicating the formation of greater TiO_2 crystallites and enhancement of crystallization. The crystallinity of TiO_2 was quantitatively evaluated via the intensity of the first diffraction peak of the anatase.

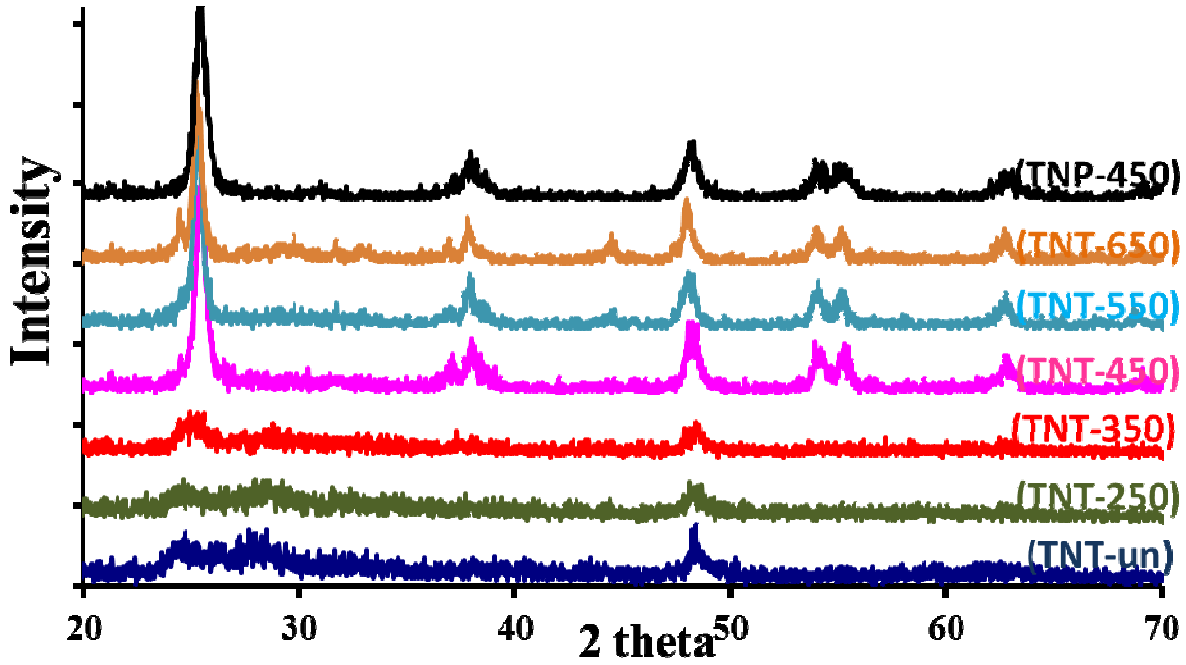

Fig. 1: XRD patterns of prepared TiO_2 nanoparticles (TNPs) and TiO_2 nanotubes (TNTs)

Fig. 2 displays HRTEM images and electron diffraction patterns of the prepared TiO_2 nanoparticles, TiO_2 nanotubes uncalcined and calcined at different temperatures for 4 h further confirm that single nanoparticle is single crystal. It can be seen that the high-purity nanotubes were produced through the hydrothermal treatment of TiO_2, the image of TNT calcinated at 250 °C, the outer diameter of the tubular structures was around 15 nm and the length was around 70 nm, the wall of nanotube was two layers in one side and three layers in another side, it can be calculated that the interlayer spacing was about 1–1.5 nm. The nanotubes are flexible and can be well-dispersed, TNT-350 was still pure nanotube, while for TNT-450, partial shorter tubular structure was presented, and in TNT-550 inner diameter of TNT decreased and many rod-like materials were formed. In TNT-650, almost all nanotubes transformed to rod-like particles and many particles could be aggregated together form polycrystalline nanoparticle.

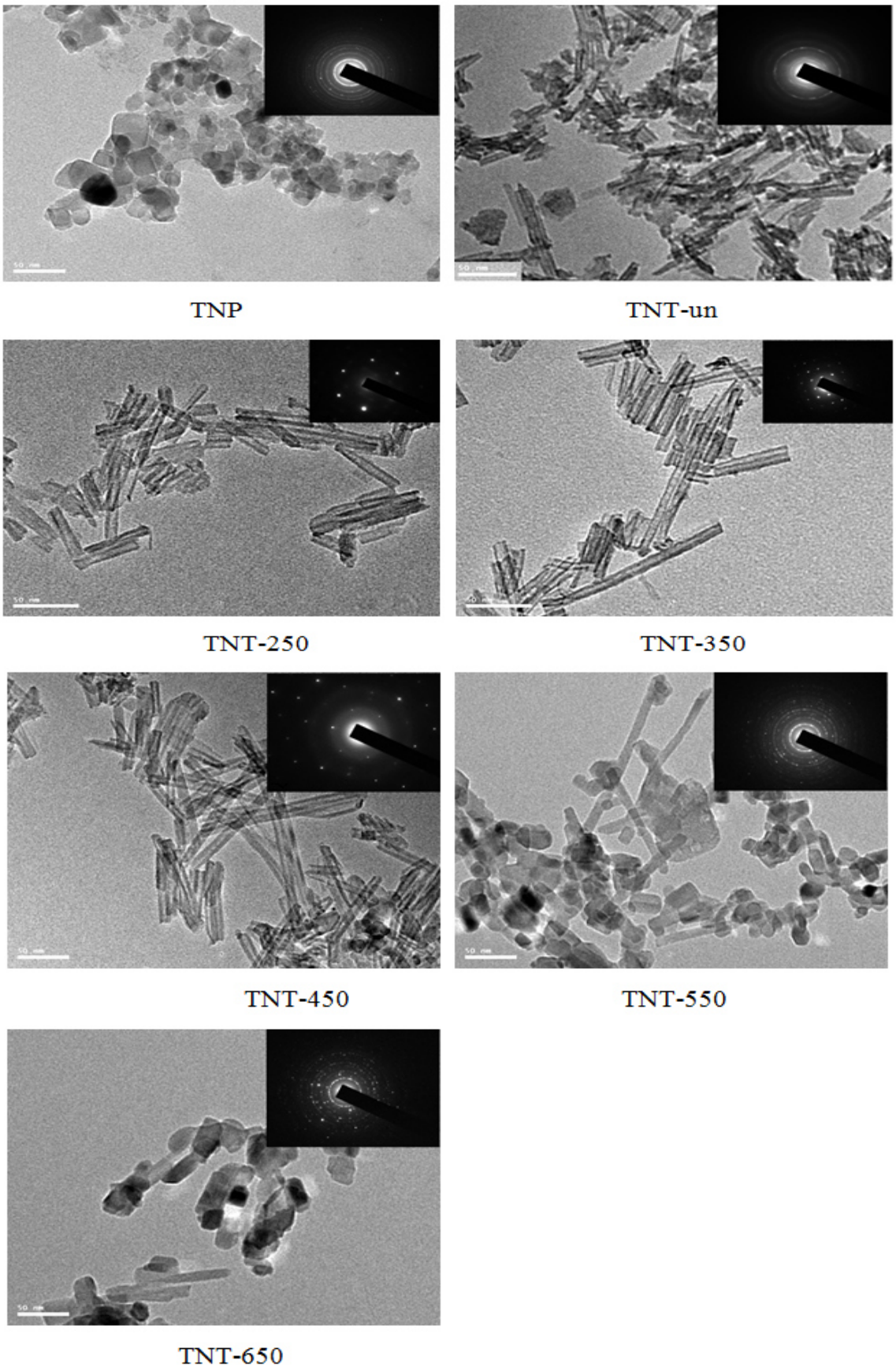

Fig. 2: HRTEM images and electron diffraction patterns of prepared TiO_2 nanoparticles (TNPs) and TiO_2 nanotubes (TNTs)

Fig. 3 showed the TG curves of the prepared TiO_2 nanoparticles uncalcined and calcined at 450 ºC for 2 h, TiO_2 nanotubes calcined at 250 and 650 ºC for 4 h, the total weight losses of uncalcined TNP and TNT-250 in the temperature of 50–300 ◦C was about 10 and 20% respectively, which was ascribed to the water desorption. The higher weight losses of TNT for interlayer space of TNTs wall, and the higher calcination temperature 650 ºC for 4 h of TNTs resulted the disappear of interlayer space of TNTs where all nanotubes transformed to rod-like particles as agreement with TEM imges.

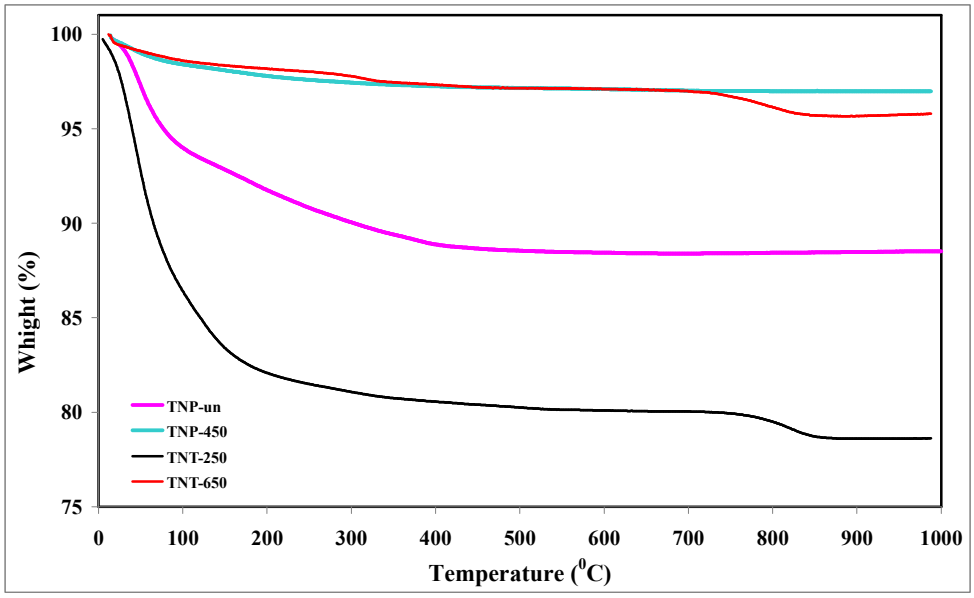

Fig. 3: the TG curves of prepared TNPs and TNTs

Fig.4 showed the Raman spectra of TNP and TNTs. The observed Raman peaks at 144 cm^{-1}, 198 cm^{-1}, 400 cm^{-1}, 519 cm^{-1}, 640 cm^{-1} were attributed to the typical anatase active modes, and the bands in the 275 cm^{-1}, 448 cm^{-1} and 668 cm^{-1} were assigned to the titanate nanotubes (Qian, 2005). According to Cortés-Jácome (2007), the band at 917 cm^{-1} was related to Ti–O–Na vibration in the interlayer regions of nanotube walls, in our Raman spectra, the peak at 917 cm^{-1} was not detected, indicative of the thorough exchange of H^+ with Na^+ in the process of acid-exchange. For the TNT-un and TNT-250, there were pure titanate, and for TNT-350 the spectra of anatase began to appear, therefore the TNT-350 contain mixed phase of titanate and anatase, which cannot be distinguished in XRD patterns. For TNT-450, the intensity of anatase peak increased rapidly. Further increase the calcination temperature from 550 to 650 ºC, the intensity of anatase peak enhanced evidently, reflecting the crystalline degree became better.

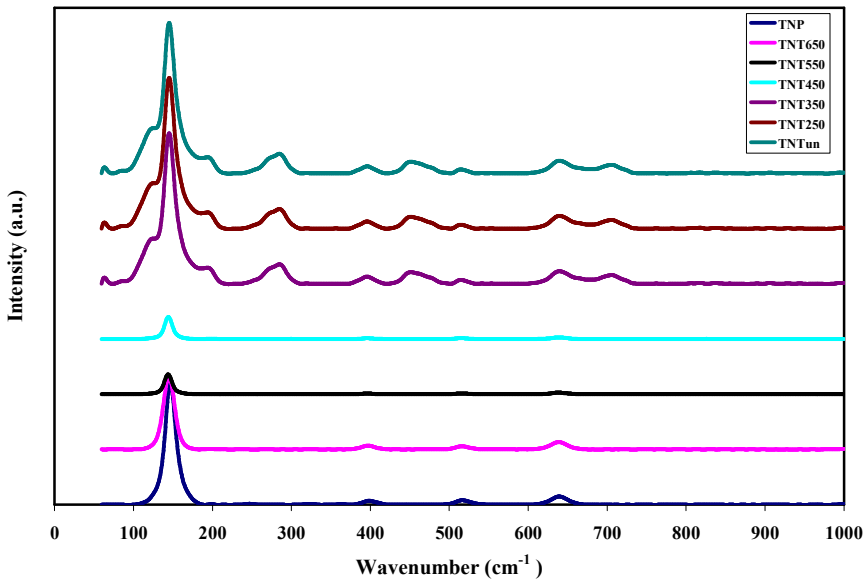

Fig. 4: Raman spectra of prepared TNP and TNTs.

Fig. 5 depicted the dependence of specific surface area of TNTs on calcination temperature. The TNT uncalcined own a high surface area of 267 m^2/g, and the calcination under 350 °C did not cause the change of surface area, which indicated that the tubular structure of TNT was stable under the calcination temperature of 350 °C. Increasing the calcination temperature from 450 to 650 °C, the surface area decreased sharply (S450 = 195.5 m^2/g, S550 = 124.5 m^2/g, S650 = 103.3 m^2/g), note that the specific surface area of prepared TiO_2 nanoparticles calcined at 450 ºC for 2 h about 200 m^2/g, and the structure of nanotube enhance the surface area of prepared TiO_2 nanoparticles markedly.

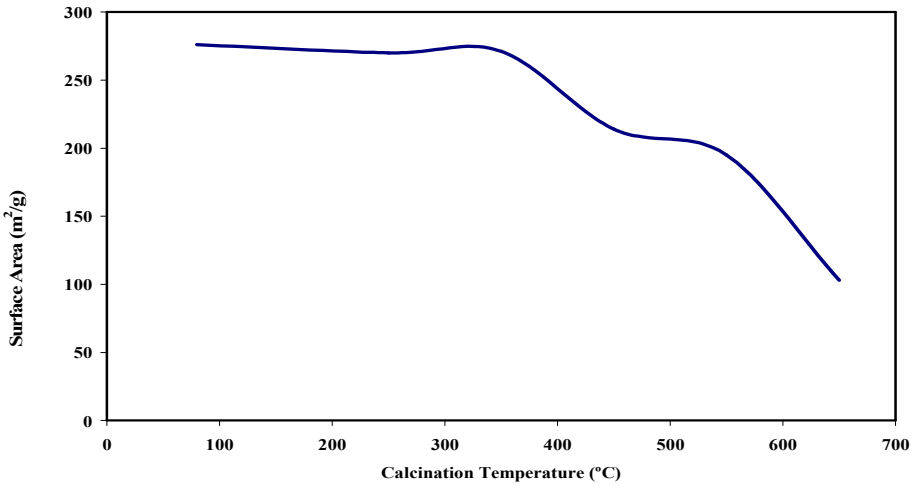

Fig. 5: Dependence of specific surface area of TNTs on calcination temperature.

Fig. 6 presents the FT-IR spectra of TNPs and TNTs obtained under different calcination temperature. All of the presented spectra exhibit, in the n(OH) region, one band with a maximum at 3585–3700 cm^{-1}, which characterize the stretching vibrations of Ti^{4+}–OH surface hydroxyl groups (Qamar et. al. 2008). The broad band (from about 800 till 400 cm^{-1}) was assigned to Ti–O and Ti–O–Ti skeletal frequency region. The bands observed at 1630–1640 cm^{-1} can be assigned to molecular water bending mode (Maira et. al. 2001). In the range of 3300–3500 cm^{-1} the bands due to adsorbed water and hydroxyl groups can be observed in all of the spectra.
The intensity gradually decreases as the temperature increases. It is noted that, this band absorption of TNT-550 and TNT-650 is much weaker than that of the others samples. The above facts indicate higher temperature results in the loss of surface hydroxyl groups, which have been recognized to play an important role in the photocatalytic process. The hydroxyl groups capture holes on illuminated photocatalysts and form active hydroxyl radicals, and then oxidize the adsorbed molecules.

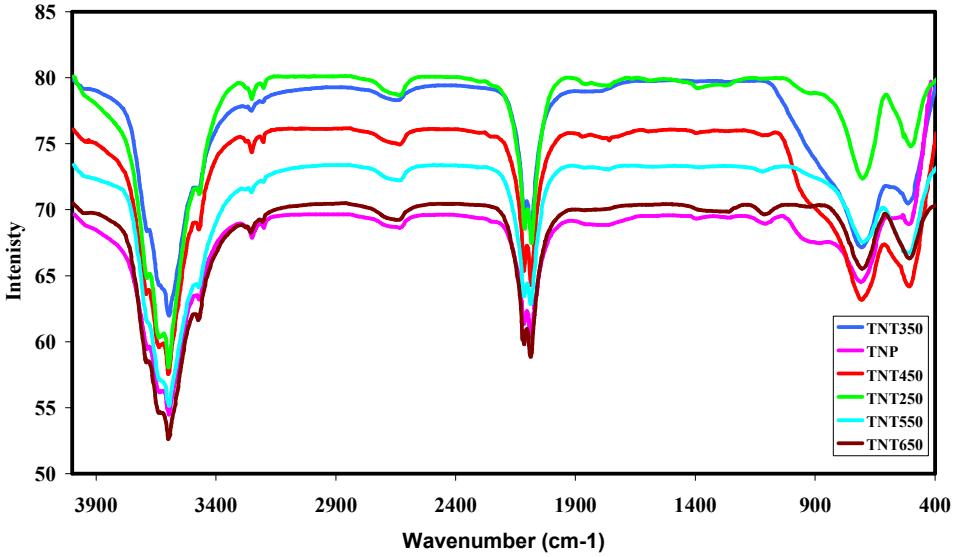

Fig. 7: FT-IR spectra of TNPs and TNTs obtained under different calcination temperature.

Fig. 8 presents UV–vis diffuse reflectance spectra of TNP-450, TNT-350 and TNT-450. The TNTs spectra, exhibit a similar course and are blue shifted for about 20 nm relative to TNPs. This indicates the increase of the band gap energy. The Eg values were calculated from the $(F(R)h\upsilon)^{1/2}$ versus hυ plots, where F(R)=(1-R)/2R (Todorova et. al. 2006). The absorption edges were found to be 378 nm, which value corresponds to the band gap energy of Eg=3.28eV for TNT.The absorption edge and Eg determined for TNP-450 were 399 nm and 3.10 eV, respectively. This value is consistent with the already published results (Todorova et. al. 2008). The literature data Wang et. al, (2006) concerning band gap of titanate nanotubes are in consistent. Some researchers found that Eg of TNT was higher than that of anatase, whereas others reported in verse relation. For example, Yu and Yu, (2006) reported that Eg of TNTs prepared from rutile ranged from 3.03 to 3.15 eV, depending on the hydrothermal treatment time. Such low values of Eg were associated with a high rutile content in the prepared samples. Khan et. al., (2009) found the band gap of 3.1 eV, whereas Wang et. al., (2006) determined the Eg=3.6eV. Bavykin et. al. (2005 & 2004) reported Eg value as high as 3.87eV.

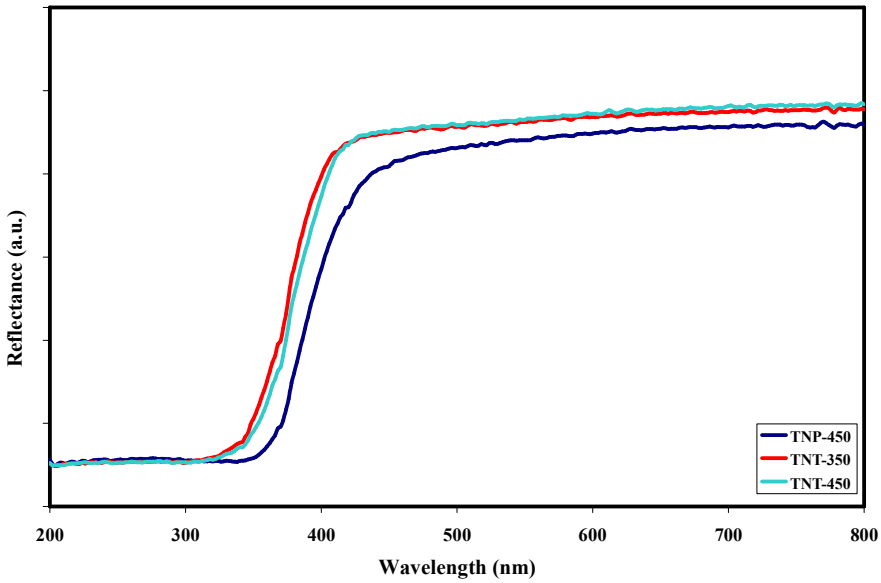

Fig. 8: UV–vis diffuse reflectance spectra of TNP-450, TNT-350 and TNT-450.

Fig. 9 A shows the Ti 2p and O 1s XPS spectra of TNPs and TNTs obtained under different calcination temperatures. The signal of TNT-un, TNT-250 and TNT-350 can be fitted with two components, one at 458.38 eV for the Ti 2p3/2 and another one at 464.18 eV for the Ti 2p1/2, corresponding to the Ti 2p spin-orbit components of Ti(IV) surface species. In comparison with TNP-450, TNTs samples at high calcination temperatures show a shift of Ti 2p (IV) binding energies of 0.3, 0.5, and 0.6 eV for calcination temperatures of 450, 550, and 650 °C, respectively. This shift to higher binding energy could be explained by the increase in effective positive charge around Ti(IV) surface species. According to the literature, the typical Ti 2p bands of pure titania are located at 458.6 and 463.8 eV (Kraeutler and Bard, 1978). This negative shift may be attributed due to the presence of residual sodium in titanate sample. The electron density on the Ti is increased because of the presence of sodium ions carrying positive charge, as a result of formation of linkages between sodium and titania as Na O Ti. Shifts in binding energies can be caused by changes in the bond environment (i.e. strength of bond). It does represent the strengthening and shortening of the Ti O bond in the titanate crystal structure (Guo et. al. 2007) as compared to TiO_2. Additionally, calculated from the results of XPS spectra for the O1s region. The individual peaks of O 1s at 529.88 eV and Ti 2p at 458.38 and 464.18 eV can be clearly seen in the high-resolution spectra, which mean that chemical state of the sample is Ti^{4+} bonded with oxygen (Ti^{4+}–O). In the meantime, the spectra show a trace amount of carbon (C 1s), which should be ascribed to the adventitious hydrocarbon from the XPS sample preparation.

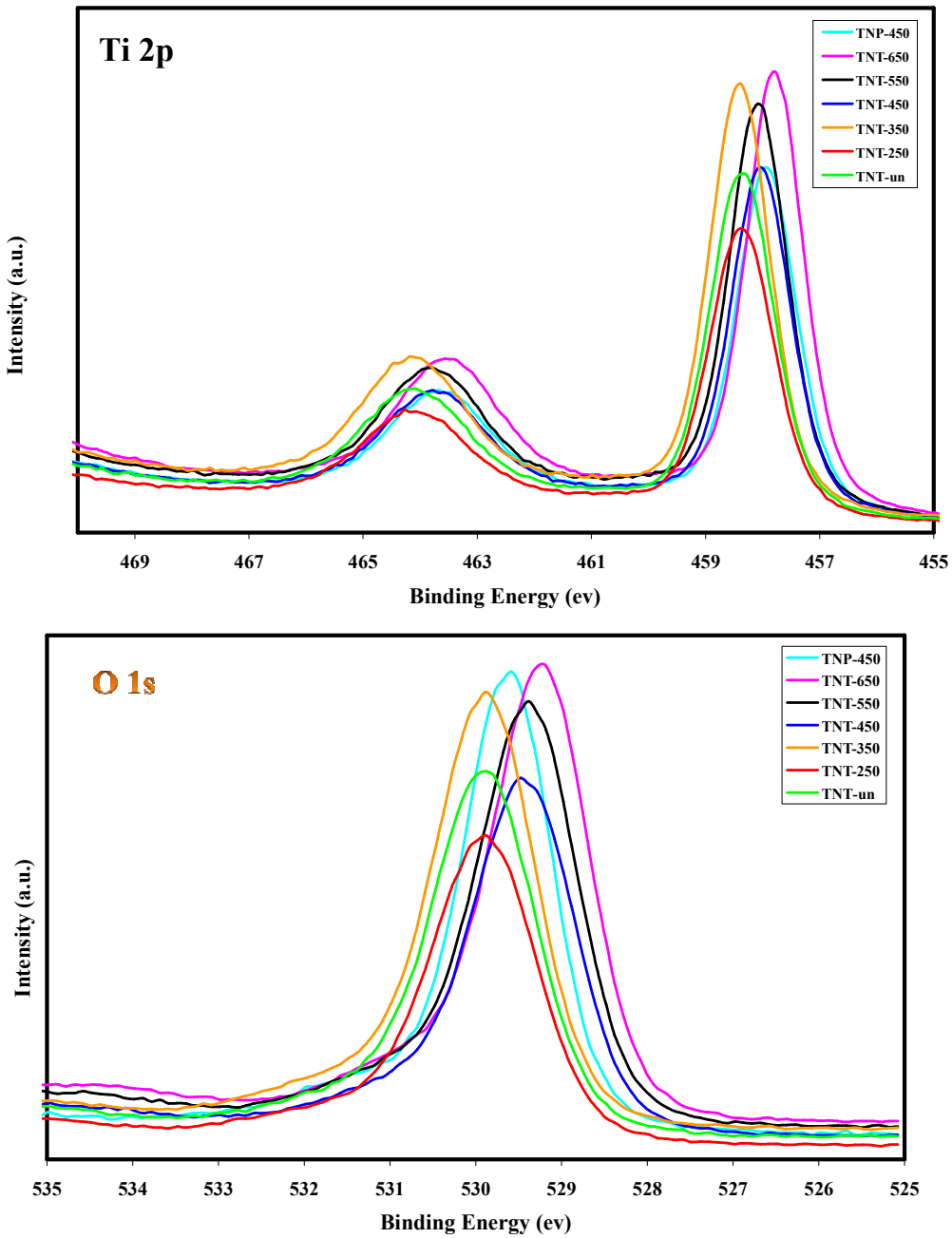

Fig. 9: The Ti 2p and O 1s XPS spectra of TNPs and TNTs obtained under different calcination temperatures.

3.2. Photocatalytic Activity

The photocatalytic degradation of aqueous phenol over the catalysts is compiled in Fig. 10. For phenol degradation overall photocatalysts, aqueous phenol concentration continuously diminished with UV irradiation, indicating that the synthesized TiO_2 nanoparticles and TiO_2 nanotubes are effective photocatalysts. However, phenol degradation efficiency varied with the structural properties of the catalysts. After UV irradiation for 300 min, phenol removal were found to be 42.5%, 49.3%, 60.9% and 65.2% for TNP, TNT-250, TNT-350 and TNT-450 reflecting the highest photocatalytic activity of TNT-450 catalysts examined.

In principle, the photocatalytic activity is closely linked to the structural properties of the photocatalyst, such as crystallinity, crystalline phase composition and specific surface area. The higher phenol degradation rate of TNT-450 compared to TNT-250 is attributed to the higher photocatalytic activity of its titanate structure (Costa and Prado, 2009).

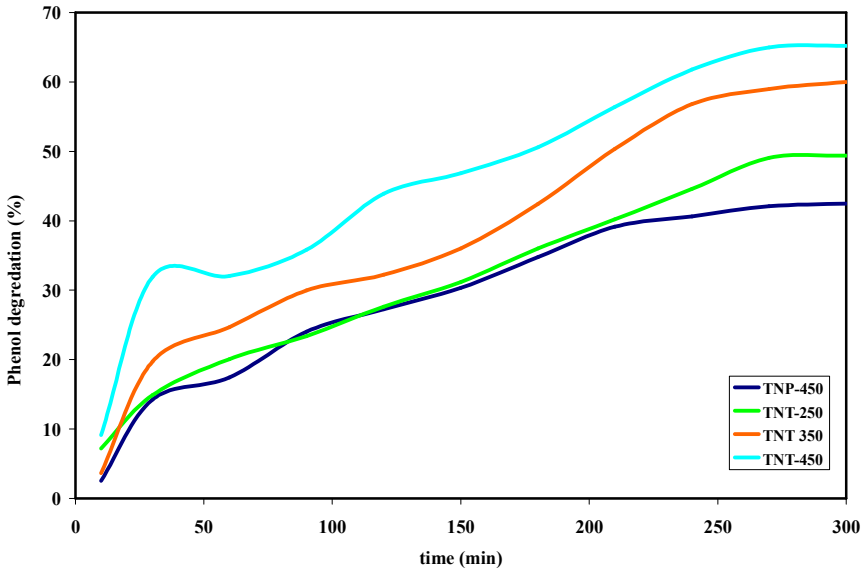

Fig. 10: The photocatalytic degradation of aqueous phenol over the catalysts.

4. CONCLUSIONS

Single crystal titanated was successfully prepared using modified hydrothermal method. Results obtained reveal that the calcination temperatures has a great influence on the physicochemical properties and photocatalytic activity of the TiO_2 calcinated at lower than 450 °C, the obtained titanate possesses much higher specific area than TNPs. Especially TNTs at 450 °C sample is the most efficient photocatalyst in this study. The superior activity can be attributed to the crystal structure, the high surface area and large pore volume, the abundant hydroxyl groups. Calcinated at high temperature (550 °C or 650 °C), the obtained samples show the poorer photocatalytic activity.

REFERENCES

Aqeel M. Ali, Ali H. Al-Mowali , (2013) "Doping, Vacancy formation and Substitutional Effects on Semiconductor Selectivity of Rutile TiO_2 Crystal" Chemistry and Materials Research www.iiste.org, ISSN 2224-3224, Vol.3 No.2,

Bavykin D.V., Friedrich J.M., Walsh F.C., (2006) "Protonated titanates and TiO_2 nanostructured materials: synthesis, properties and applications", Advanced Materials 18, 2807–2824.

Bavykin D.V., Parmon V.N., Lapkin A.A., Walsh F.C., (2004) "The effect of hydrothermal conditions on the mesoporous structure of TiO2 nanotubes, Journal of Materials Chemistry 14, 3370–3377.

Bavykin D.V., Gordeev S.N., Moskalenko A.V., Lapkin A.A., Walsh F.C., (2005) "Apparent two-dimensional behavior of TiO_2 nanotubes revealed by light absorption and luminescence", J. Phys. Chem. B, 109, 8565–8569.

Chen X.B., Mao S.S., Titanium dioxide nanomaterials: synthesis, properties, modifications, and applications, Chem. Rev. 107 (2007) 2891–2959.

Cortés-Jácome M.A., Ferrat-Torres G., Flores Ortiz L.F., Angeles-Chávez C., López-Salinas E., Escobar J., Mosqueira M.L., Toledo-Antonio J.A., (2007) "In situ thermo-Raman study of titanium oxide nanotubes", Catalysis Today 126, 248–255.

Costa L.L., Prado A.G.S., (2009) "TiO_2 nanotubes as recyclable catalyst for efficient photocatalytic degradation of indigo carmine dye", J. Photochem. Photobiol. A: Chem. 201, 45–49.

Feist T.P., Mocarski S.J., Davies P.K., Jacobson A.J., Lewandowski J.T., (1988) "Formation of TiO_2 by proton exchange and thermolysis of several alkali metal titanate structure, Solid State Ionics, 28, 1338–1343.

Guo G., He N., Z. Wang H., Gu F., Han D., (2007) "Synthesis of titania and titanate nanomaterials and their application in environmental analytical chemistry", Talanta72, 1687–1692.

Kasuga T., Hiramatsu M., Hoson A., Sekino T., Niihara K., (1998) "Formation of titanium oxide nanotube" Langmuir, 14, 3160–3163.

Kasuga T., Hiramatsu M., Hoson A., Sekino T., Niihara K., (1999) "Titania nanotubes prepared by chemical processing", Advanced Materials 11, 1307–1311.

Khan M.A., Han D.H., Yang O., (2009) "Enhanced photo response to wards visible light in Ru doped titania nanotube", Appl.Surf.Sci., 255, 3687–3690.

Kraeutler B., Bard A.J., (1978) "Heterogenous photocatalytic synthesis of methane from acetic acid—new Kolbe reaction pathway", J.Am.Chem.Soc.100, 2239–2240.

Li Shi Wang, Ming Wei Xiao, Xin Jian Huang, Yan Dan Wu, (2009) "Synthesis, characterization, and photocatalytic activities of titanate nanotubes surface-decorated by zinc oxide nanoparticles", Journal of Hazardous Materials, 161, 49–54.
Lin C.H., Chao J.H., Liu C.H., Chang J.C., Wang F.C., (2008) "Effect of calcination temperature on the structure of a Pt/TiO_2 nanofiber and its photocatalytic activity in generating H_2", Langmuir 24, 9907–9915.
Maira A.J., Coronado J.M., Augugliaro V., Yeung K.L., Conesa J.C., J.Soria, (2001) "Fourier transform infrared study of the performance of nanostructured TiO_2 particles for the photocatalytic oxidation of gaseous toluene", J.Catal. 202, 413–420.
Morgado E. Jr., de Abreu M.A.S., Moure G.T., Marinkovic B.A., Jardim P.M., Araujo A.S. (2007) "Characterization of nanostructured titanates obtained by alkali treatment of TiO_2-anatases with distinct crystal sizes, Chem. Mater. 19, 665–676.
Nalwa H.S., (2000) "Handbook of Nanostrucutred Materials and Nanotechnology" Academic Press, New York,.
Ou H.H., Lo S.L., (2007) "Review of titania nanotubes synthesized via the hydrothermal treatment: fabrication, modification and application", Separation and Purification Technology 58, 179–191.
Qamar M., Yoon C.R. , Oh H.J., Lee N.H., Park K., Kim D.H., Lee K.S., Lee W.J., Kim S.J., (2008) "Preparation, photocatalytic activity of nanotubes obtained from titanium dioxide", Catalysis Today 131, 3–14.
Qian L., Du Z.L., Yang S.Y., Jin Z.S., (2005) "Raman study of titania nanotube by soft chemical process", Journal of Molecular Structure 749, 103–107.
S.S. Kanmani, K. Ramachandran, (2012) "Synthesis and characterization of TiO2/ZnO core/shell nanomaterials for solar cell applications", Renewable Energy, 43, 149-156.
Sun K.C., Chen Y.C., Kuo M.Y., Wang H.W., Lu Y.F., Chung J.C., Liu Y.C., Zeng Y.Z., (2011) "Synthesis and characterization of highly ordered TiO2 nanotube arrays for hydrogen generation via water splitting", Materials Chemistry and Physics, 129, 35–39.
Todorova N., Giannakopoulou T., Romanos G., Vaimakis T., JiaguoYu,C. Trapalis, (2008) "Preparation of fluorine-doped TiO_2 photocatalysts with controlled crystalline structure". Int. J. Photoenergy ,Article ID 534038 (2008)9, doi:10. 1155/2008/534038.
Wang N., Lin H., Li J., Yang X., Chi B., Lin Ch., (2006) "Effect of annealing temperature on phase transition and optical property of titanate nanotubes prepared by ion exchange approach ,J.Alloy Compd. 424, 311–314.
Wu D., Liu J., Zhao X.N., Li A.D., Chen Y.F., Ming N.B., (2006) "Sequence of events for the formation of titanate nanotubes, nanofibers, nanowires, and nanobelts", Chem. Mater. 18, 547–553.
Yu J., Yu H., (2006) "Facile synthesis and characterization of novel nanocomposites of titanate nanotubes and rutile nanocrystals", Mater.Chem.Phys. 100, 507–512.
Zhang J.H., Xiao X., Nan J.M., (2010) "Hydrothermal-hydrolysis synthesis and photocatalytic properties of nano-TiO_2 with an adjustable crystalline structure", J. Hazard. Mater. 176, 617–622.

The IISTE is a pioneer in the Open-Access hosting service and academic event management. The aim of the firm is Accelerating Global Knowledge Sharing.

More information about the firm can be found on the homepage:
http://www.iiste.org

CALL FOR JOURNAL PAPERS

There are more than 30 peer-reviewed academic journals hosted under the hosting platform.

Prospective authors of journals can find the submission instruction on the following page: http://www.iiste.org/journals/ All the journals articles are available online to the readers all over the world without financial, legal, or technical barriers other than those inseparable from gaining access to the internet itself. Paper version of the journals is also available upon request of readers and authors.

MORE RESOURCES

Book publication information: http://www.iiste.org/book/

IISTE Knowledge Sharing Partners

EBSCO, Index Copernicus, Ulrich's Periodicals Directory, JournalTOCS, PKP Open Archives Harvester, Bielefeld Academic Search Engine, Elektronische Zeitschriftenbibliothek EZB, Open J-Gate, OCLC WorldCat, Universe Digtial Library , NewJour, Google Scholar